Proceedings of the 7th IFAC Symposium on Robust Control Design
The International Federation of Automatic Control
Aalborg, Denmark, June 20-22, 2012

Robust observer-based fault detection and isolation in the standard control problem framework

Arne Wahrburg, * **Saman Khodaverdian,** * **Jürgen Adamy** *

* *Institute of Automatic Control; Control Theory & Robotics Lab; Technische Universität Darmstadt, Germany (e-mail: {wahrburg, jadamy}@rtr.tu-darmstadt.de).*

Abstract: This paper deals with the design of robust fault detection and isolation observers where only a single observer is employed to isolate different faults. To this end, the problem of parameterizing such observers is shown to be equivalent to designing a structurally constrained controller in the standard control problem framework. Thereby, the problem is reformulated as a well known classical control problem, which enables the use of existing tools to optimize robustness with respect to arbitrary exogenous disturbances. To account for parametric uncertainties, an approximate model matching approach is used.

Keywords: robust fault diagnosis, observer-based fault detection and isolation, standard control problem, structurally constrained control, model matching

1. INTRODUCTION

Safe and reliable operation is a crucial requirement for technical systems, especially due to increasing complexity. Therefore, research on model-based fault diagnosis has been receiving a lot of attention over the past years (cf. e.g. Chen and Patton (1999), Isermann (2005)).

Among other techniques, observer-based approaches have proven to be applicable in the presence of parametric uncertainties as well as exogenous disturbances (Ding (2008)). All practical systems are subject to both phenomena, which is why increasing robustness is frequently pursued (e.g. Mazars et al. (2007), Li et al. (2011), Glover and Varga (2011)). Instead of mere detection, *fault isolation* aims at identifying which specific faults are acting on a system. There are various approaches to achieve this using banks of dedicated or generalized observers (Frank and Ding (1997), Ibaraki et al. (2001)). In Liu and Si (1997), *fault isolation observers* (FIOs) were introduced. These schemes enable to isolate faults by using only a single observer, which significantly reduces the computational effort. Especially in applications where computational resources are limited, an FIO approach can therefore have considerable advantages and enable online implementations. The FIOs are parameterized to assign a specific structure to the residuals, creating a diagonal transfer matrix relating faults and residuals. As shown in Wahrburg and Adamy (2012), the FIO design can thus be interpreted as the dual problem to non-interacting control first introduced by Falb and Wolovich (1967). Since several degrees of freedom are used to achieve isolation, robustness is hard to accomplish in FIO schemes. If more sensors than potential faults are available, LMI-based schemes have been proposed to optimize disturbance attenuation (Jaimoukha et al. (2006), Chen and Nagarajaiah (2007), Wahrburg and Adamy (2012)).

In this paper, we focus on square systems with only as many sensors as possible faults. Obviously robustness is harder to achieve in this case because less information is available. However, we point out that there are remaining degrees of freedom in the observer design and the proper use of these may be interpreted as a structurally constrained control problem. To this end, we reformulate the design of an FIO in the standard control problem framework, similar as Chen (2008) does for fault detection and estimation. Due to the structural constraints, the optimization problem is non-convex. Recently, solvers relying on non-smooth optimization techniques such as HIFOO (Gumussoy et al. (2009), Arzelier et al. (2011)) have been successfully applied to this kind of problems (cf. e.g. Rezac and Hurak (2011)). In this contribution we show the applicability of HIFOO for the design of FIOs with robustness regarding both exogenous disturbances as well as uncertain parameters.

Hence, the paper is structured as follows. Section 2 summarizes some basic mathematical tools and notation and gives a proper problem statement. In Section 3, robust FIOs with respect to external disturbances are designed by reformulating the problem as a standard control problem. Based on these results, robustness with respect to parametric uncertainties is considered in Section 4. To show the applicability of the results, an example demonstrating robust fault isolation for a spring-mass-damper system is included in Section 5 before a conclusion is given.

2. PRELIMINARIES

2.1 Notation and mathematical background

A matrix of zeros with appropriate dimensions is written as $\mathbf{0}$ while $\boldsymbol{I}_n$ denotes the identity matrix of order n. For a matrix $\boldsymbol{M} \in \mathbb{R}^{n\times m}$, $\boldsymbol{m}_i$ represents the i-th column of $\boldsymbol{M}$.

Positive and negative definiteness of a matrix $\boldsymbol{X} = \boldsymbol{X}^{\mathsf{T}} \in \mathbb{R}^{n\times n}$ is denoted by $\boldsymbol{X} \succ \boldsymbol{0}$ and $\boldsymbol{X} \prec \boldsymbol{0}$, respectively. In symmetric matrices, $\star$ symbolizes symmetric elements. For a square matrix $\boldsymbol{Q} \in \mathbb{R}^{n\times n}$, its hermitian part is written as $\mathrm{He}\,(\boldsymbol{Q}) = \boldsymbol{Q}+\boldsymbol{Q}^{\mathsf{T}}$. Its eigenvalues are denoted by $\lambda_i(\boldsymbol{Q})$, the spectrum is written as $\sigma(\boldsymbol{Q})$ and the *spectral abscissa* refers to $\max_i \{\mathfrak{Re}\,(\lambda_i)\}$. A linear dynamical system $\dot{\boldsymbol{x}} = \boldsymbol{A}\boldsymbol{x} + \boldsymbol{B}\boldsymbol{u}$, $\boldsymbol{y} = \boldsymbol{C}\boldsymbol{x} + \boldsymbol{D}\boldsymbol{u}$ is abbreviated as $(\boldsymbol{A}, \boldsymbol{B}, \boldsymbol{C}, \boldsymbol{D})$ or $(\boldsymbol{A}, \boldsymbol{B}, \boldsymbol{C})$ if $\boldsymbol{D} = \boldsymbol{0}$. In the paper we use the Bounded Real Lemma (Boyd et al. (1994)), which is given below.

Lemma 1. Given a stable linear system $(\boldsymbol{A}, \boldsymbol{B}, \boldsymbol{C}, \boldsymbol{D})$ with transfer matrix $\boldsymbol{G}(s) = \boldsymbol{C}\,(s\boldsymbol{I} - \boldsymbol{A})^{-1}\,\boldsymbol{B} + \boldsymbol{D}$. Then $\|\boldsymbol{G}(s)\|_\infty < \gamma$ holds if and only if there exists $\gamma > 0$ and a real symmetric matrix $\boldsymbol{X} \succ \boldsymbol{0}$ such that

$$\begin{bmatrix} \mathrm{He}\,(\boldsymbol{X}\boldsymbol{A}) & \boldsymbol{X}\boldsymbol{B} & \boldsymbol{C}^{\mathsf{T}} \\ \star & -\gamma\boldsymbol{I} & \boldsymbol{D}^{\mathsf{T}} \\ \star & \star & -\gamma\boldsymbol{I} \end{bmatrix} \prec \boldsymbol{0}.$$

2.2 Problem statement

We consider linear systems described by

$$\dot{\boldsymbol{x}} = \boldsymbol{A}\boldsymbol{x} + \boldsymbol{B}\boldsymbol{u} + \boldsymbol{E}\boldsymbol{f} + \boldsymbol{B}_d\boldsymbol{d}, \qquad \text{(1a)}$$

$$\boldsymbol{y} = \boldsymbol{C}\boldsymbol{x} + \boldsymbol{D}_d\boldsymbol{d}, \qquad \text{(1b)}$$

with $\boldsymbol{x} \in \mathbb{R}^n$, $\boldsymbol{u} \in \mathbb{R}^{n_u}$, $\boldsymbol{f} \in \mathbb{R}^{n_f}$, $\boldsymbol{d} \in \mathbb{R}^{n_d}$, and $\boldsymbol{y} \in \mathbb{R}^{n_y}$. The matrices are of appropriate dimensions. We only consider actuator faults with fault input matrix $\boldsymbol{E}$, since sensor faults can be recast as pseudo-actuator faults (Park et al. (1994)). Parametric uncertainties, which might be caused by imprecise modeling or linearization errors, are taken into account by $\boldsymbol{A} \in \mathcal{A}$ and $\boldsymbol{B} \in \mathcal{B}$. We assume matrices $\boldsymbol{A}_l, \boldsymbol{B}_l$, $l = 0, \ldots, N$ defining $\mathcal{A}$ and $\mathcal{B}$, which we elaborate on further in Section 4. Arbitrary *disturbances* $\boldsymbol{d}$ might be caused by exogenous inputs or nonlinearities. The *faults* $\boldsymbol{f}$ are to be detected and isolated by means of an FIO, which is of the structure

$$\dot{\hat{\boldsymbol{x}}} = \boldsymbol{A}_0\hat{\boldsymbol{x}} + \boldsymbol{B}_0\boldsymbol{u} + \boldsymbol{L}\,(\boldsymbol{y} - \boldsymbol{C}\hat{\boldsymbol{x}})\,, \qquad \text{(2a)}$$

$$\boldsymbol{r} = \boldsymbol{V}\,(\boldsymbol{y} - \boldsymbol{C}\hat{\boldsymbol{x}})\,. \qquad \text{(2b)}$$

Therein, $\boldsymbol{A}_0 \in \mathcal{A}$ and $\boldsymbol{B}_0 \in \mathcal{B}$ are the nominal system matrices assumed for the plant. To achieve robust fault isolation with respect to both disturbances and parametric uncertainties, the proposed design scheme can be divided into three steps as depicted in Fig. 1. First, the observer gains $(\boldsymbol{L}_0, \boldsymbol{V}_0)$ are parameterized in Section 3 such that the transfer function $\boldsymbol{G}_{\boldsymbol{rf}}(s)$ relating faults and residuals $\boldsymbol{r} \in \mathbb{R}^{n_f}$ in the nominal system is rendered diagonal, i.e.,

$$\boldsymbol{G}_{\boldsymbol{rf}}(s) = \mathrm{diag}\left(g_{r_1f_1}(s), \ldots, g_{r_{n_f}f_{n_f}}(s)\right). \qquad (3)$$

The transfer functions $g_{r_if_i}(s)$ describing the relation of fault f_i and residual r_i are of the form

$$g_{r_if_i}(s) = \frac{z_{i0}}{s^{\delta_i} + q_{i\delta_i-1}s^{\delta_i-1} + \ldots + q_{i1}s + q_{i0}}. \qquad (4)$$

Therein, the *fault detectability indices* δ_i are defined as

$$\delta_i = \min\left\{k\colon \boldsymbol{C}\boldsymbol{A}_0^{k-1}\boldsymbol{e}_i \neq \boldsymbol{0},\, k = 1, 2, \ldots\right\}. \qquad (5)$$

Furthermore, we define $\delta = \sum_{k=1}^{n_f} \delta_k$ and the *fault detectability matrix* $\boldsymbol{D}^* \in \mathbb{R}^{n_y\times n_f}$ as

$$\boldsymbol{D}^* = \left[\boldsymbol{C}\boldsymbol{A}_0^{\delta_1-1}\boldsymbol{e}_1 \;\cdots\; \boldsymbol{C}\boldsymbol{A}_0^{\delta_{n_f}-1}\boldsymbol{e}_{n_f}\right], \qquad (6)$$

and focus on square systems with $n_y = n_f$ while the results can be extended to non-square systems. The systems fulfill the following assumptions.

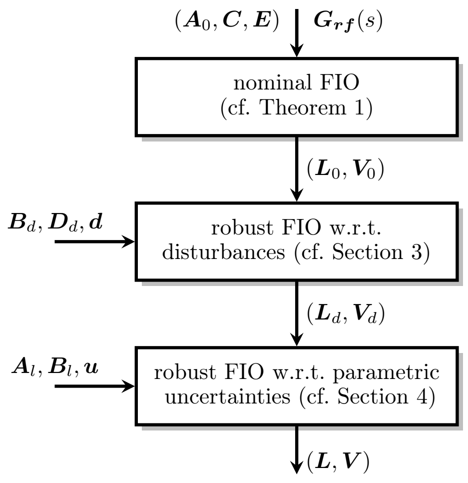

Fig. 1. Structure of the proposed design scheme

Assumption 1. $\boldsymbol{A}_l$ is Hurwitz for all $l = 0, \ldots, N$.

Assumption 2. The pair $(\boldsymbol{A}_0, \boldsymbol{C})$ is observable.

Assumption 3. The system $(\boldsymbol{A}_0, \boldsymbol{E}, \boldsymbol{C})$ is minimum phase.

Assumption 4. The system is fault isolable by means of a static FIO, i.e., $\boldsymbol{D}^*$ is (left-)invertible.

After the observer $(\boldsymbol{L}_0, \boldsymbol{V}_0)$ has been found based on the nominal plant and the specified $\boldsymbol{G}_{\boldsymbol{rf}}(s)$, robustness of the FIO with respect to exogenous disturbances $\boldsymbol{d}$ is optimized using $(\boldsymbol{L}_0, \boldsymbol{V}_0)$ as an initial solution in the second step, which is described in detail in Section 3. The resulting observer parameterization $(\boldsymbol{L}_d, \boldsymbol{V}_d)$ can then be used as an initial solution for the problem of approximate model matching, which is used to increase robustness in case of parametric uncertainties (cf. Section 4) while preserving disturbance attenuation. As a result, we obtain the final observer parameterization $(\boldsymbol{L}, \boldsymbol{V})$.

3. ROBUST FAULT ISOLATION FOR DISTURBED SYSTEMS

In this section we focus on fault isolation with optimized disturbance rejection. We first assume $\boldsymbol{A} = \boldsymbol{A}_0$ and $\boldsymbol{B} = \boldsymbol{B}_0$ but nevertheless keep the notation $\boldsymbol{A}$, $\boldsymbol{A}_0$ and $\boldsymbol{B}$, $\boldsymbol{B}_0$ to distinguish between plant and observer matrices.

First we recall the parameterization $(\boldsymbol{L}_0, \boldsymbol{V}_0)$ of an observer achieving perfect fault isolation for an undisturbed system without parametric uncertainties. The free parameters q_{ij} can be chosen by pole placement techniques for each transfer channel, while z_{i0} can be selected to specify a specific static gain.

Theorem 1. Given a system (1) with $\boldsymbol{d} = \boldsymbol{0}$ and $\boldsymbol{A} = \boldsymbol{A}_0$, $\boldsymbol{B} = \boldsymbol{B}_0$ fulfilling Assumptions 1–4. With

$$\boldsymbol{M}\,(\boldsymbol{q}_{ij}) = \begin{bmatrix} \left(\boldsymbol{A}_0^{\delta_1}\boldsymbol{e}_1 + \sum_{k=0}^{\delta_1-1} q_{1k}\boldsymbol{A}_0^k\boldsymbol{e}_1\right)^{\mathsf{T}} \\ \vdots \\ \left(\boldsymbol{A}_0^{\delta_{n_f}}\boldsymbol{e}_{n_f} + \sum_{k=0}^{\delta_{n_f}-1} q_{n_fk}\boldsymbol{A}_0^k\boldsymbol{e}_{n_f}\right)^{\mathsf{T}} \end{bmatrix}^{\mathsf{T}},$$

$$\boldsymbol{N}\,(\boldsymbol{z}_{i0}) = \mathrm{diag}\left(z_{10}, \ldots, z_{n_f0}\right),$$

an observer parameterized by $\boldsymbol{L}_0 = \boldsymbol{M}(\boldsymbol{q}_{ij})\,\boldsymbol{D}^{*-1}$ and $\boldsymbol{V}_0 = \boldsymbol{N}(\boldsymbol{z}_{i0})\,\boldsymbol{D}^{*-1}$ results in a diagonal transfer matrix $\boldsymbol{G}_{\boldsymbol{rf}}(s) = \mathrm{diag}\left(g_{r_1 f_1}(s), \ldots, g_{r_{n_f} f_{n_f}}(s)\right)$ with

$$g_{r_i f_i}(s) = \frac{z_{i0}}{s^{\delta_i} + q_{1\delta_i - 1} s^{\delta_i - 1} + \ldots + q_{i0}}.$$

Proof 1. The theorem is a special case of a result presented in Wahrburg and Adamy (2012) with $n_y = n_f$. Thus the proof, which is based on the classical result by Falb and Wolovich (1967), is omitted here.

In case of $n_y > n_f$, the observer gains can be tuned to minimize $\|\boldsymbol{G}_{\boldsymbol{rd}}(s)\|_\infty$ while preserving the selected eigenvalues of $\boldsymbol{A}_0 - \boldsymbol{L}_0\boldsymbol{C}$ (cf. Jaimoukha et al. (2006), Chen and Nagarajaiah (2007), Wahrburg and Adamy (2012)). Thereby, the influence of disturbances onto the residuals is attenuated, since perfect disturbance decoupling can only be achieved under very restrictive conditions (Chen and Patton (1999)). However, if only $n_y = n_f$ sensors are available the only remaining degrees of freedom are the coefficients q_{ij} and z_{i0} describing the transfer functions $g_{r_i f_i}(s)$. To the best of the authors' knowledge, the problem of achieving robustness in square systems by properly placing the poles of $\boldsymbol{G}_{\boldsymbol{rf}}(s)$ has not been considered so far. Therefore, we have to solve

$$\underset{q_{ij}, z_{i0}}{\text{minimize}}\ \gamma_{rd}, \quad \text{s.t.}$$

$$\boldsymbol{L}_d = \boldsymbol{M}(\boldsymbol{q}_{ij})\,\boldsymbol{D}^{*-1}, \tag{7a}$$

$$\boldsymbol{V}_d = \boldsymbol{N}(\boldsymbol{z}_{i0})\,\boldsymbol{D}^{*-1}, \tag{7b}$$

$$\|\boldsymbol{G}_{\boldsymbol{rd}}(s)\|_\infty < \gamma_{rd}. \tag{7c}$$

Due to the isolation property, the observer gains are structurally constrained, rendering the optimization problem non-convex. While this can be tackled by path-following methods (Ostertag (2008)), the key idea to our approach is to reformulate (7) as a standard control problem with structural constraints. The standard control problem

$$\mathcal{P}: \begin{cases} \dot{\widetilde{\boldsymbol{x}}} = \widetilde{\boldsymbol{A}}\widetilde{\boldsymbol{x}} + \widetilde{\boldsymbol{B}}_1\boldsymbol{w} + \widetilde{\boldsymbol{B}}_2\widetilde{\boldsymbol{u}}, \\ \boldsymbol{z} = \widetilde{\boldsymbol{C}}_1\widetilde{\boldsymbol{x}} + \widetilde{\boldsymbol{D}}_{11}\boldsymbol{w} + \widetilde{\boldsymbol{D}}_{12}\widetilde{\boldsymbol{u}}, \\ \widetilde{\boldsymbol{y}} = \widetilde{\boldsymbol{C}}_2\widetilde{\boldsymbol{x}} + \widetilde{\boldsymbol{D}}_{21}\boldsymbol{w} + \widetilde{\boldsymbol{D}}_{22}\widetilde{\boldsymbol{u}}, \end{cases} \tag{8a}$$

$$\mathcal{K}: \widetilde{\boldsymbol{u}} = \widetilde{\boldsymbol{K}}\widetilde{\boldsymbol{y}}, \tag{8b}$$

with generalized plant $\mathcal{P}$ and controller $\mathcal{K}$ is depicted in Fig. 2. Combining plant and observer state vector as $\widetilde{\boldsymbol{x}} = [\boldsymbol{x}^\mathsf{T}\ \hat{\boldsymbol{x}}^\mathsf{T}]^\mathsf{T}$ and disturbances and inputs as a generalized input $\boldsymbol{w} = [\boldsymbol{d}^\mathsf{T}\ \boldsymbol{u}^\mathsf{T}]^\mathsf{T}$, the generalized plant can be described by

$$\widetilde{\boldsymbol{A}} = \begin{bmatrix} \boldsymbol{A} & \boldsymbol{0} \\ \boldsymbol{0} & \boldsymbol{A}_0 \end{bmatrix}, \ \widetilde{\boldsymbol{B}}_1 = \begin{bmatrix} \boldsymbol{B}_d & \boldsymbol{B} \\ \boldsymbol{0} & \boldsymbol{B}_0 \end{bmatrix}, \ \widetilde{\boldsymbol{B}}_2 = \begin{bmatrix} \boldsymbol{0} & \boldsymbol{0} \\ \boldsymbol{0} & \boldsymbol{I}_n \end{bmatrix}, \tag{9a}$$

$$\widetilde{\boldsymbol{C}}_1 = \boldsymbol{0}, \qquad \widetilde{\boldsymbol{D}}_{11} = \boldsymbol{0}, \qquad \widetilde{\boldsymbol{D}}_{12} = \begin{bmatrix} \boldsymbol{I}_{n_f} & \boldsymbol{0} \end{bmatrix}, \tag{9b}$$

$$\widetilde{\boldsymbol{C}}_2 = [\boldsymbol{C}\ \ {-\boldsymbol{C}}], \widetilde{\boldsymbol{D}}_{21} = [\boldsymbol{D}_d\ \ \boldsymbol{0}], \quad \widetilde{\boldsymbol{D}}_{22} = \boldsymbol{0}, \tag{9c}$$

with the measurable output $\widetilde{\boldsymbol{y}} = \boldsymbol{y} - \hat{\boldsymbol{y}}$ and performance output $\boldsymbol{z} = \boldsymbol{r}$. We propose to use the observer gains $\boldsymbol{L}_d$ and $\boldsymbol{V}_d$ in the generalized controller as

$$\widetilde{\boldsymbol{K}} = \begin{bmatrix} \boldsymbol{V}_d^\mathsf{T} & \boldsymbol{L}_d^\mathsf{T} \end{bmatrix}^\mathsf{T}. \tag{10}$$

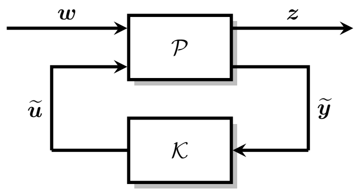

Fig. 2. Standard control problem

The observer gains must match the structural constraints imposed by (7) to achieve isolation. Contrary to that, constraints are imposed in the standard control problem as zero elements in the generalized controller. In the following, we reformulate the generalized plant (9) and controller (10) to match this structure. Therefore, we first partition the matrix $\boldsymbol{M}(\boldsymbol{q}_{ij})$ given in Theorem 1 as

$$\boldsymbol{M}(\boldsymbol{q}_{ij}) = \boldsymbol{M}_\alpha + \boldsymbol{M}_\beta \boldsymbol{Q}_L(\boldsymbol{q}_{ij}) \tag{11}$$

with $\boldsymbol{M}_\beta$ as shown in (12) (cf. bottom of page) and

$$\boldsymbol{M}_\alpha = \begin{bmatrix} \boldsymbol{A}_0^{\delta_1}\boldsymbol{e}_1 & \cdots & \boldsymbol{A}_0^{\delta_{n_f}}\boldsymbol{e}_{n_f} \end{bmatrix}, \tag{13a}$$

$$\boldsymbol{Q}_L(\boldsymbol{q}_{ij}) = \begin{bmatrix} q_{1\delta_1-1} & 0 & \cdots\ \cdots\ \cdots & & 0 \\ \vdots & \vdots & & & \vdots \\ q_{10} & 0 & \cdots\ \cdots\ \cdots & & 0 \\ 0 & q_{2\delta_2-1} & 0\ \ \cdots\ \cdots & & 0 \\ \vdots & \vdots & & & \vdots \\ 0 & q_{20} & 0\ \ \cdots\ \cdots & & 0 \\ & & \ddots & & \\ 0 & \cdots & \cdots\ \cdots & 0 & q_{n_f\delta_{n_f}-1} \\ \vdots & & & \vdots & \vdots \\ 0 & \cdots & \cdots\ \cdots & 0 & q_{n_f0} \end{bmatrix}. \tag{13b}$$

Note that $\boldsymbol{M}_\alpha$ and $\boldsymbol{M}_\beta$ only depend on the plant itself while the remaining degrees of freedom available in the FIO design are included in $\boldsymbol{Q}_L(\boldsymbol{q}_{ij}) = \boldsymbol{Q}_L$. In a similar manner, we partition the post-filter matrix $\boldsymbol{V}_d$ as

$$\boldsymbol{V}_d = \boldsymbol{Q}_V(\boldsymbol{z}_{i0})\,\boldsymbol{D}^{*-1} = \mathrm{diag}\left(z_{10}, \ldots, z_{n_f0}\right)\boldsymbol{D}^{*-1}. \tag{14}$$

Inserting the partitioned observer gain $\boldsymbol{L}_d$ from (7a) into the observer dynamics (2a) yields

$$\begin{aligned} \dot{\hat{\boldsymbol{x}}} = {} & \boldsymbol{M}_\alpha\boldsymbol{D}^{*-1}\boldsymbol{C}\boldsymbol{x} + \left(\boldsymbol{A}_0 - \boldsymbol{M}_\alpha\boldsymbol{D}^{*-1}\boldsymbol{C}\right)\hat{\boldsymbol{x}} + \boldsymbol{B}_0\boldsymbol{u} + \ldots \\ & + \boldsymbol{M}_\alpha\boldsymbol{D}^{*-1}\boldsymbol{D}_d\boldsymbol{d} + \boldsymbol{M}_\beta\boldsymbol{Q}_L\boldsymbol{D}^{*-1}(\boldsymbol{y} - \hat{\boldsymbol{y}}), \end{aligned} \tag{15}$$

which results in the new generalized plant matrices

$$\widetilde{\boldsymbol{A}} = \begin{bmatrix} \boldsymbol{A} & \boldsymbol{0} \\ \boldsymbol{M}_\alpha\boldsymbol{D}^{*-1}\boldsymbol{C} & \boldsymbol{A}_0 - \boldsymbol{M}_\alpha\boldsymbol{D}^{*-1}\boldsymbol{C} \end{bmatrix}, \tag{16a}$$

$$\widetilde{\boldsymbol{B}}_1 = \begin{bmatrix} \boldsymbol{B}_d & \boldsymbol{B} \\ \boldsymbol{M}_\alpha\boldsymbol{D}^{*-1}\boldsymbol{D}_d & \boldsymbol{B}_0 \end{bmatrix}. \tag{16b}$$

The associated generalized controller is given by

$$\widetilde{\boldsymbol{K}} = \left[(\boldsymbol{Q}_V\boldsymbol{D}^{*-1})^\mathsf{T} \quad (\boldsymbol{M}_\beta\boldsymbol{Q}_L\boldsymbol{D}^{*-1})^\mathsf{T}\right]^\mathsf{T}. \tag{17}$$

The next step is to interpret the matrix $\boldsymbol{M}_\beta$ as part of the generalized plant dynamics and $\boldsymbol{D}^{*-1}$ as a virtual modification of the measurement. As a result of this operation, all structural constraints have been shifted into

$$\boldsymbol{M}_\beta = \begin{bmatrix} \boldsymbol{A}_0^{\delta_1-1}\boldsymbol{e}_1 & \boldsymbol{A}_0^{\delta_1-2}\boldsymbol{e}_1 & \cdots & \boldsymbol{A}_0\boldsymbol{e}_1 & \boldsymbol{e}_1 & \boldsymbol{A}_0^{\delta_2-1}\boldsymbol{e}_2 & \cdots & \boldsymbol{A}_0\boldsymbol{e}_2 & \boldsymbol{e}_2 & \cdots & \cdots & \boldsymbol{A}_0^{\delta_{n_f}-1}\boldsymbol{e}_{n_f} & \cdots & \boldsymbol{A}_0\boldsymbol{e}_{n_f} & \boldsymbol{e}_{n_f} \end{bmatrix} \tag{12}$$

fixed zero elements in the generalized controller. Because we assume $\boldsymbol{A}=\boldsymbol{A}_0$ and $\boldsymbol{B}=\boldsymbol{B}_0$ in this section, $\boldsymbol{u}$ has no influence on neither the observer error nor the residuals. This implies $\|\boldsymbol{G}_{\boldsymbol{zw}}(s)\|_\infty = \|\boldsymbol{G}_{\boldsymbol{rd}}(s)\|_\infty$ and we can state the following lemma.

Lemma 2. Optimization problem (7) can equivalently be formulated as a structurally constrained standard control problem with matrices

$$\widetilde{\boldsymbol{A}} = \begin{bmatrix} \boldsymbol{A} & \boldsymbol{0} \\ \boldsymbol{M}_\alpha \boldsymbol{D}^{*-1}\boldsymbol{C} & \boldsymbol{A}_0 - \boldsymbol{M}_\alpha \boldsymbol{D}^{*-1}\boldsymbol{C} \end{bmatrix},$$

$$\widetilde{\boldsymbol{B}}_1 = \begin{bmatrix} \boldsymbol{B}_d & \boldsymbol{B} \\ \boldsymbol{M}_\alpha \boldsymbol{D}^{*-1}\boldsymbol{D}_d & \boldsymbol{B}_0 \end{bmatrix},\ \widetilde{\boldsymbol{B}}_2 = \begin{bmatrix} \boldsymbol{0} & \boldsymbol{0} \\ \boldsymbol{0} & \boldsymbol{M}_\beta \end{bmatrix},$$

$$\widetilde{\boldsymbol{C}}_1 = \boldsymbol{0},\ \widetilde{\boldsymbol{D}}_{11} = \boldsymbol{0},\ \widetilde{\boldsymbol{D}}_{12} = \begin{bmatrix} \boldsymbol{I}_{n_f} & \boldsymbol{0} \end{bmatrix},\ \widetilde{\boldsymbol{D}}_{22} = \boldsymbol{0},$$

$$\widetilde{\boldsymbol{C}}_2 = \begin{bmatrix} \boldsymbol{D}^{*-1}\boldsymbol{C} & -\boldsymbol{D}^{*-1}\boldsymbol{C} \end{bmatrix},\ \widetilde{\boldsymbol{D}}_{21} = \begin{bmatrix} \boldsymbol{D}^{*-1}\boldsymbol{D}_d & \boldsymbol{0} \end{bmatrix},$$

and generalized controller

$$\widetilde{\boldsymbol{K}} = \begin{bmatrix} \boldsymbol{Q}_V^\mathsf{T} & \boldsymbol{Q}_L^\mathsf{T} \end{bmatrix}^\mathsf{T},$$

which minimizes $\|\boldsymbol{G}_{\boldsymbol{zw}}(s)\|_\infty$.

The optimization problem posed in Lemma 2 might result in very small values for z_{i0}, since fault sensitivity is not considered. To overcome this problem, we specify a static gain of 1 for the transfer channels $g_{r_i f_i}(s)$ by imposing $z_{i0} = q_{i0}$ in (4). This condition constrains the minimum singular value of $g_{r_i f_i}(s)$ at $s = 0$ and thus improves low frequency fault sensitivity compared to Lemma 2. The generalized controller can be written as

$$\widetilde{\boldsymbol{K}} = \begin{bmatrix} \boldsymbol{Q}_V \\ \boldsymbol{Q}_L \end{bmatrix} = \boldsymbol{S}\boldsymbol{Q}_L, \boldsymbol{S} = \begin{bmatrix} \boldsymbol{\Phi} \\ \boldsymbol{I}_\delta \end{bmatrix}, \boldsymbol{\Phi} = \begin{bmatrix} \boldsymbol{\varphi}_1 & \cdots & \boldsymbol{\varphi}_{n_f} \end{bmatrix}^\mathsf{T}. \quad (18)$$

Therein, $\boldsymbol{\varphi}_i = [0 \cdots 0\ 1\ 0 \cdots 0]^\mathsf{T}$ are unit vectors with element 1 in the $\sum_{k=1}^{i} \delta_k$-th row. Interpreting $\boldsymbol{S}$ as part of the generalized plant, we can state the following theorem.

Theorem 2. The generalized control problem with structurally constrained static output feedback as stated in Lemma 2 with modified matrices

$$\widetilde{\boldsymbol{B}}_2 = \begin{bmatrix} \boldsymbol{0} & \boldsymbol{0} \\ \boldsymbol{0} & \boldsymbol{M}_\beta \end{bmatrix} \boldsymbol{S},\ \widetilde{\boldsymbol{D}}_{12} = \begin{bmatrix} \boldsymbol{I}_{n_f} & \boldsymbol{0} \end{bmatrix} \boldsymbol{S},\ \widetilde{\boldsymbol{K}} = \boldsymbol{Q}_L$$

equivalently describes optimization problem (7) with $g_{r_i f_i}(s=0) = 1\,\forall i = 1, \ldots, n_f$.

Theorem 2 enables to directly apply solvers for the standard problem of structurally constrained static output feedback such as HIFOO (Gumussoy et al. (2009), Arzelier et al. (2011)) to the robust FIO design.

Apart from fault sensitivity and disturbance attenuation, detection speed has to be considered in fault diagnosis systems. To this end, the observer eigenvalues should fulfill $\mathfrak{Re}(\lambda_i) < \mu \forall \lambda_i \in \sigma(\boldsymbol{A}_0 - \boldsymbol{L}_d\boldsymbol{C})$, where μ is a negative real scalar. This condition on the spectral abscissa of $\boldsymbol{A}_0 - \boldsymbol{L}_d\boldsymbol{C}$ ensures a sufficient observer convergence rate. To account for this in the robust FIO design we utilize HIFOO's capability to simultaneously handle several generalized plants and impose different constraints on them. Therefore, we set up a second generalized plant only concerned with the eigenvalues of $\boldsymbol{A}_0 - \boldsymbol{L}_d\boldsymbol{C}$. It is parameterized by

$$\overline{\boldsymbol{A}} = \boldsymbol{A}_0 - \boldsymbol{M}_\alpha \boldsymbol{D}^{*-1}\boldsymbol{C}, \quad (19a)$$

$$\overline{\boldsymbol{B}}_2 = -\boldsymbol{M}_\beta, \quad (19b)$$

$$\overline{\boldsymbol{C}}_2 = \boldsymbol{D}^{*-1}\boldsymbol{C}, \quad (19c)$$

and all other elements of the generalized plant set to $\boldsymbol{0}$. Note that (19) is controlled by the same controller $\widetilde{\boldsymbol{K}}$ as the plant set up in Theorem 2. The optimization is then executed with the H_∞ norm of the first plant as the optimization objective with a spectral abscissa smaller than μ for the second plant as a constraint.

In presence of parametric uncertainties, the approach described above could easily be extended to attenuate the influence of the input $\boldsymbol{u}$ onto the residuals $\boldsymbol{r}$ by using $\boldsymbol{A} \neq \boldsymbol{A}_0$ and $\boldsymbol{B} \neq \boldsymbol{B}_0$. Note however, that undesired cross-couplings between faults f_i and residuals r_j, $i \neq j$, caused by the uncertainties would not be taken into account. This is dealt with in the following section.

4. ROBUST FAULT DETECTION AND ISOLATION USING REFERENCE MODELS

To account for parametric uncertainties in the system model, model matching techniques can be used. As proposed in Zhong et al. (2003), a *reference model* is given or constructed for the nominal system. Following the optimization shown in Section 3, the relation between faults and disturbances and the generated residuals of the reference model is described by

$$\dot{\boldsymbol{x}}_\text{ref} = \boldsymbol{A}_\text{ref}\boldsymbol{x}_\text{ref} + \boldsymbol{B}_{\text{ref},f}\boldsymbol{f} + \boldsymbol{B}_{\text{ref},d}\boldsymbol{d}, \quad (20a)$$

$$\boldsymbol{r}_\text{ref} = \boldsymbol{C}_\text{ref}\boldsymbol{x}_\text{ref} + \boldsymbol{D}_{\text{ref},f}\boldsymbol{f} + \boldsymbol{D}_{\text{ref},d}\boldsymbol{d}, \quad (20b)$$

with $\boldsymbol{A}_\text{ref} = \boldsymbol{A}_0 - \boldsymbol{L}_d\boldsymbol{C}$, $\boldsymbol{B}_{\text{ref},f} = \boldsymbol{E}$, $\boldsymbol{B}_{\text{ref},d} = \boldsymbol{B}_d - \boldsymbol{L}_d\boldsymbol{D}_d$, $\boldsymbol{C}_\text{ref} = \boldsymbol{V}_d\boldsymbol{C}$, $\boldsymbol{D}_{\text{ref},f} = \boldsymbol{0}$, $\boldsymbol{D}_{\text{ref},d} = \boldsymbol{V}_d\boldsymbol{D}_d$. The basic idea then is to design a model-based residual generator that approximates the dynamics of (20) as exactly as possible in the presence of parametric uncertainties. In Mazars et al. (2007) this is achieved by a general filter, while Zhong et al. (2003) use an observer-based approach. Note that the best possible disturbance attenuation level for the nominal plant and maximum insensitivity with respect to uncertain parameters can generally not be obtained at the simultaneously. In the model matching approach, there is an inherent tradeoff between the two criteria. Furthermore, it is worth mentioning that the model matching approach is generally applicable for both fault detection and fault isolation. The solution $(\boldsymbol{L}, \boldsymbol{V})$ obtained is not structurally constrained. Whether detection or isolation is conducted only depends on the choice of the reference model.

Combining the observer dynamics (2), the reference model (20) and the plant dynamics (1) yields the overall system (21) (cf. bottom of next page) with the state vector $\boldsymbol{x}_g = [\boldsymbol{\eta}^\mathsf{T}\ \boldsymbol{x}_\text{ref}^\mathsf{T}\ \boldsymbol{x}^\mathsf{T}]^\mathsf{T}$. Therein, $\boldsymbol{\eta} = \boldsymbol{x} - \hat{\boldsymbol{x}}$ is the observer error and $\boldsymbol{z} = \boldsymbol{r} - \boldsymbol{r}_\text{ref}$ describes the difference between the generated residual and the reference model residual and $\boldsymbol{w} = [\boldsymbol{u}^\mathsf{T}\ \boldsymbol{f}^\mathsf{T}\ \boldsymbol{d}^\mathsf{T}]^\mathsf{T}$ is the input to the augmented system. Furthermore, we introduce $\Delta\boldsymbol{A}_l = \boldsymbol{A}_l - \boldsymbol{A}_0$ and $\Delta\boldsymbol{B}_l = \boldsymbol{B}_l - \boldsymbol{B}_0$ for notational purposes. Since perfect matching cannot be achieved in general, approximate model matching is pursued by solving the following optimization problem.

$$\underset{\boldsymbol{L},\boldsymbol{V}}{\text{minimize}}\ \gamma_{zw}, \quad \text{s.t.}$$

$$\|\boldsymbol{G}_{\boldsymbol{zw},l}(s)\|_\infty < \gamma_{zw}\ \forall l = 0, \ldots, N. \quad (22)$$

In Zhong et al. (2003) a solution is obtained by formulating (22) as an LMI-problem using Lemma 1. However, a blockdiagonal Lyapunov matrix is needed resulting in conservative results. Therefore we reformulate (20) as a standard control problem in the following lemma.

Lemma 3. The dynamics (21) describing the model matching problem can equivalently be formulated as a standard control problem with $\widetilde{\boldsymbol{x}} = \boldsymbol{x}_g$ using the matrices

$$\begin{aligned}
\widetilde{\boldsymbol{A}}_l &= \begin{bmatrix} \boldsymbol{A}_0 & \boldsymbol{0} & \Delta\boldsymbol{A}_l \\ \boldsymbol{0} & \boldsymbol{A}_{\mathrm{ref}} & \boldsymbol{0} \\ \boldsymbol{0} & \boldsymbol{0} & \boldsymbol{A}_0 + \Delta\boldsymbol{A}_l \end{bmatrix}, \; \widetilde{\boldsymbol{B}}_2 = \begin{bmatrix} \boldsymbol{0} & -\boldsymbol{I}_n \\ \boldsymbol{0} & \boldsymbol{0} \\ \boldsymbol{0} & \boldsymbol{0} \end{bmatrix}, \\
\widetilde{\boldsymbol{B}}_{1,l} &= \begin{bmatrix} \Delta\boldsymbol{B}_l & \boldsymbol{E} & \boldsymbol{B}_d \\ \boldsymbol{0} & \boldsymbol{B}_{\mathrm{ref},f} & \boldsymbol{B}_{\mathrm{ref},d} \\ \boldsymbol{B}_0 + \Delta\boldsymbol{B}_l & \boldsymbol{E} & \boldsymbol{B}_d \end{bmatrix}, \; \widetilde{\boldsymbol{C}}_1 = [\boldsymbol{0} \;\, -\boldsymbol{C}_{\mathrm{ref}} \;\, \boldsymbol{0}], \\
\widetilde{\boldsymbol{D}}_{11} &= [\boldsymbol{0} \;\, -\boldsymbol{D}_{\mathrm{ref},f} \;\, -\boldsymbol{D}_{\mathrm{ref},d}], \; \widetilde{\boldsymbol{D}}_{12} = [\boldsymbol{I}_{n_f} \;\, \boldsymbol{0}], \\
\widetilde{\boldsymbol{C}}_2 &= [\boldsymbol{C} \;\, \boldsymbol{0} \;\, \boldsymbol{0}], \; \widetilde{\boldsymbol{D}}_{21} = [\boldsymbol{0} \;\, \boldsymbol{0} \;\, \boldsymbol{D}_d], \; \widetilde{\boldsymbol{D}}_{22} = \boldsymbol{0}, \\
\widetilde{\boldsymbol{K}} &= \begin{bmatrix} \boldsymbol{V}^{\mathsf{T}} & \boldsymbol{L}^{\mathsf{T}} \end{bmatrix}^{\mathsf{T}}.
\end{aligned}$$

Proof 2. Computing the closed loop equations in the standard control problem using $\widetilde{\boldsymbol{u}} = \widetilde{\boldsymbol{K}}\widetilde{\boldsymbol{y}}$ and inserting the matrices proposed in Lemma 3 immediately results in (21).

Due to the formulation as a standard control problem, a solution of the approximate model matching problem (22) can be found again by using HIFOO. A minimum detection speed for the observer can be assured in a similar manner as in Section 3 by including an additional generalized plant with $\overline{\boldsymbol{A}} = \boldsymbol{A}_0$, $\overline{\boldsymbol{B}}_2 = [\boldsymbol{0} \; -\boldsymbol{I}_n]$ and $\overline{\boldsymbol{C}}_2 = \boldsymbol{C}$ and constraining its spectral abscissa. For $\mathcal{A} = \{\boldsymbol{A}_0, \ldots, \boldsymbol{A}_N\}$ and $\mathcal{B} = \{\boldsymbol{B}_0, \ldots, \boldsymbol{B}_N\}$, HIFOO is used to find an observer parameterization simultaneously achieving model matching level γ for all plants $\boldsymbol{A} \in \mathcal{A}$, $\boldsymbol{B} \in \mathcal{B}$. Therein, the solution $(\boldsymbol{L}_d, \boldsymbol{V}_d)$ obtained in Section 3 is used as an initial solution. Note that the model matching level is only guaranteed for a finite number of plants. If we are interested in all plants spanned by the convex hull of $\boldsymbol{A}_l$ and $\boldsymbol{B}_l$, i.e., $\mathcal{A} = \operatorname{conv}(\boldsymbol{A}_0, \ldots, \boldsymbol{A}_N)$ and $\mathcal{B} = \operatorname{conv}(\boldsymbol{B}_0, \ldots, \boldsymbol{B}_N)$, an additional LMI-problem using Lemma 1 has to be solved.

$$\begin{aligned}
&\underset{\boldsymbol{X}=\boldsymbol{X}^{\mathsf{T}}}{\text{minimize}} \; \gamma^*, \quad \text{s.t.} \\
&\mathbb{R}^{3n \times 3n} \ni \boldsymbol{X} \succ \boldsymbol{0}, \qquad (23a)
\end{aligned}$$

$$\begin{bmatrix} \mathrm{He}(\boldsymbol{X}\boldsymbol{A}_{g,l}) & \boldsymbol{X}\boldsymbol{B}_{g,l} & \boldsymbol{C}_g^{\mathsf{T}} \\ \star & \gamma^* \boldsymbol{I}_{n_u+n_f+n_d} & \boldsymbol{D}_g^{\mathsf{T}} \\ \star & \star & -\gamma^* \boldsymbol{I}_{n_f} \end{bmatrix} \prec \boldsymbol{0} \; \forall l = 0, \ldots, N. \qquad (23b)$$

Thereby, we compute the model matching level $\gamma^* \geq \gamma$ that is achieved for time-varying parameters inside $\mathcal{A}$ and $\mathcal{B}$. If bounds on the changing speed of the parameters are known, less conservative solutions can be found by employing parameter dependent Lyapunov matrices (Apkarian and Tuan (2000)).

5. EXAMPLE

To demonstrate the applicability of the proposed approaches, we combine the results of Sections 3 and 4 and use them to design a robust FIO for a spring-mass-damper system shown in Fig. 3. The system dynamics are

$$\boldsymbol{A}_0 = \begin{bmatrix} 0 & 1 & 0 & 0 \\ -\dfrac{k_1 + k_{2,0}}{m_1} & -\dfrac{d_2}{m_1} & \dfrac{k_{2,0}}{m_1} & \dfrac{d_2}{m_1} \\ 0 & 0 & 0 & 1 \\ \dfrac{k_{2,0}}{m_2} & \dfrac{d_2}{m_2} & -\dfrac{k_{2,0}}{m_2} & -\dfrac{d_2}{m_2} \end{bmatrix}, \qquad (24a)$$

$$\boldsymbol{B}_0 = \begin{bmatrix} 0 & 0 \\ 1/m_1 & 0 \\ 0 & 0 \\ 0 & 1/m_2 \end{bmatrix}, \; \boldsymbol{E} = \boldsymbol{B}_0, \; \boldsymbol{C} = \begin{bmatrix} -1 & 0 & 1 & 0 \\ 0 & 0 & 1 & 0 \end{bmatrix}, \qquad (24b)$$

with $m_1 = 5$kg, $m_2 = 4$kg, $k_1 = 20$N/m, $d_2 = 1.8$Ns/m, and an uncertain parameter $k_2 \in \{k_{2,0} = 1.8\text{N/m}, k_{2,1} = 0.9k_{2,0}, k_{2,2} = 1.1k_{2,0}\}$. An initial FIO is designed specifying observer eigenvalues of $\sigma(\boldsymbol{A}_0 - \boldsymbol{L}_0\boldsymbol{C}) = \{-3.2 \pm \jmath 1.0, -3.6, -3.8\}$ resulting in $\gamma_{rd,0} = 15.83$. The first optimization step (cf. Section 3) minimizes the influence of the disturbances onto the residuals. Constraining the spectral abscissa with an upper limit of $\mu = -1.2$, the resulting observer parameterization $(\boldsymbol{L}_d, \boldsymbol{V}_d)$ achieves $\gamma_{rd,d} = 5.79$. In Fig. 4(a), the Bode diagram for the initial observer $(\boldsymbol{L}_0, \boldsymbol{V}_0)$ and the optimized $(\boldsymbol{L}_d, \boldsymbol{V}_d)$ is shown for the nominal plant demonstrating the decreased worst case disturbance gain. In the second optimization step (cf. Section 4) a model matching level of $\gamma_{zw} = 0.67$ with $\gamma_{rd} = 6.19$ is achieved by the optimized $(\boldsymbol{L}, \boldsymbol{V})$ compared to $\gamma_{zw,d} = 0.86$ for $(\boldsymbol{L}_d, \boldsymbol{V}_d)$. In Fig. 4(b), the evaluation of the residuals is shown over time for a parameter value of $k_2 = k_{2,2}$. We compare our initial guess $(\boldsymbol{L}_0, \boldsymbol{V}_0)$ (dashed) and the final optimization results $(\boldsymbol{L}, \boldsymbol{V})$ (solid). Under a constant input signal $\boldsymbol{u}(t) = [0.5 \; -0, 8]^{\mathsf{T}}$ and a disturbance $\boldsymbol{d}(t) = [-0.03 \;\, 0.02\eta(t)]^{\mathsf{T}}$ where $\eta(t)$ is white gaussian noise with power 1 it is obvious that $(\boldsymbol{L}, \boldsymbol{V})$ is less sensitive to the disturbances. Fault 2 occurring after 2 seconds is readily isolated by both observers. However, the optimized observer reduces cross-couplings, i.e., $r_1(t)$ is less affected by the occurrence of f_2. Therefore fault 1 (after 10s) can safely be isolated by $(\boldsymbol{L}, \boldsymbol{V})$ in contrast to $(\boldsymbol{L}_0, \boldsymbol{V}_0)$.

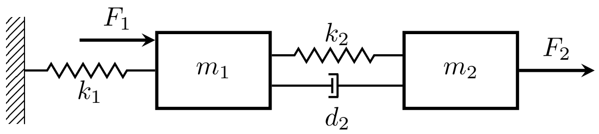

Fig. 3. Spring-mass-damper system

$$\dot{\boldsymbol{x}}_g = \underbrace{\begin{bmatrix} \boldsymbol{A}_0 - \boldsymbol{L}\boldsymbol{C} & \boldsymbol{0} & \Delta\boldsymbol{A}_l \\ \boldsymbol{0} & \boldsymbol{A}_{\mathrm{ref}} & \boldsymbol{0} \\ \boldsymbol{0} & \boldsymbol{0} & \boldsymbol{A}_0 + \Delta\boldsymbol{A}_l \end{bmatrix}}_{\boldsymbol{A}_{g,l}} \boldsymbol{x}_g + \underbrace{\begin{bmatrix} \Delta\boldsymbol{B}_l & \boldsymbol{E} & \boldsymbol{B}_d - \boldsymbol{L}\boldsymbol{D}_d \\ \boldsymbol{0} & \boldsymbol{B}_{\mathrm{ref},f} & \boldsymbol{B}_{\mathrm{ref},d} \\ \boldsymbol{B}_0 + \Delta\boldsymbol{B}_l & \boldsymbol{E} & \boldsymbol{B}_d \end{bmatrix}}_{\boldsymbol{B}_{g,l}} \boldsymbol{w}, \qquad (21a)$$

$$\boldsymbol{z} = \underbrace{[\boldsymbol{V}\boldsymbol{C} \quad -\boldsymbol{C}_{\mathrm{ref}} \quad \boldsymbol{0}]}_{\boldsymbol{C}_g} \boldsymbol{x}_g + \underbrace{[\boldsymbol{0} \quad -\boldsymbol{D}_{\mathrm{ref},f} \quad \boldsymbol{V}\boldsymbol{D}_d - \boldsymbol{D}_{\mathrm{ref},d}]}_{\boldsymbol{D}_g} \boldsymbol{w}. \qquad (21b)$$

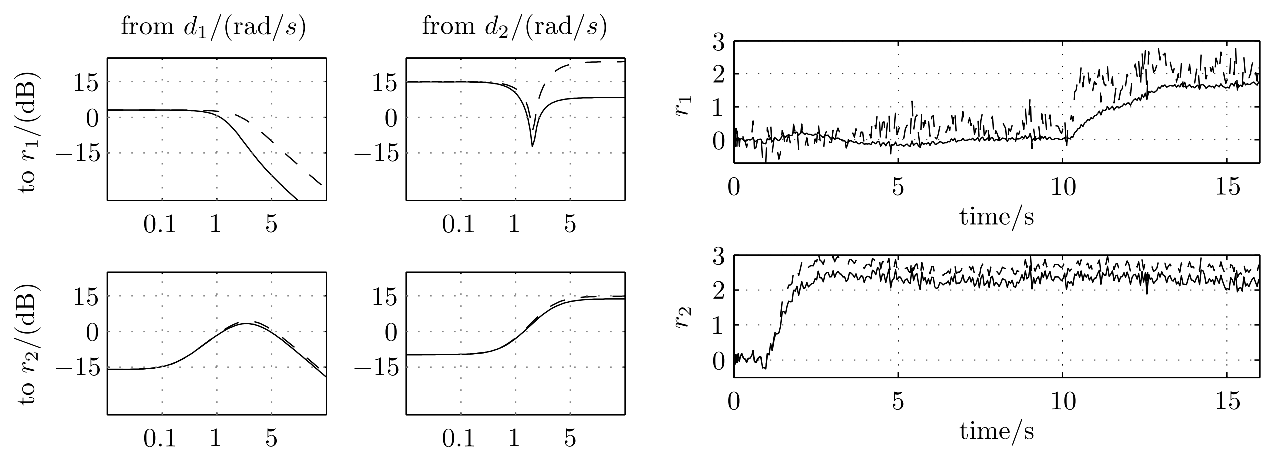

(a) $\boldsymbol{G_{rd}}(s)$ for $(\boldsymbol{L}_0, \boldsymbol{V}_0)$ (−−) and $(\boldsymbol{L}_d, \boldsymbol{V}_d)$ (−)

(b) Residuals of $(\boldsymbol{L}_0, \boldsymbol{V}_0)$ (−−) and $(\boldsymbol{L}, \boldsymbol{V})$ (−)

Fig. 4. Simulation results

6. CONCLUSION

In this contribution, we showed that the design of FIOs can be interpreted as a structurally constrained standard control problem. Therefore, it is possible to optimize disturbance rejection by properly placing the observer eigenvalues for the nominal system. By solving an approximate model matching problem, robustness with respect to parametric uncertainties can be increased in both fault detection and isolation problems. The design scheme is successfully applied to a spring-mass-damper system.

ACKNOWLEDGEMENTS

This work was supported by the Deutsche Telekom Stiftung (`www.telekom-stiftung.de`).

REFERENCES

Apkarian, P. and Tuan, H.D. (2000). Parameterized LMIs in control theory. *SIAM J. Control Optim.*, 38(4), 1241–1264.

Arzelier, D., Deaconu, G., Gumussoy, S., and Henrion, D. (2011). H_2 for HIFOO. In *Proc. of COIA'11*.

Boyd, S., El Ghaoui, L., Feron, E., and Balakrishnan, V. (1994). *Linear Matrix Inequalities in System and Control Theory*. SIAM.

Chen, B. and Nagarajaiah, S. (2007). Linear-matrix-inequality-based robust fault detection and isolation using the eigenstructure assignment method. *J. Guid. Cont. Dynam.*, 30(6), 1831–1835.

Chen, J. (2008). Formulating and solving robust fault diagnosis problems based on a H_∞ setting. In *Proc. of IFAC WC'08*, 7259–7264.

Chen, J. and Patton, R.J. (1999). *Robust Model-Based Fault Diagnosis for Dynamic Systems*. Kluwer Academic Publishers.

Ding, S.X. (2008). *Model-based Fault Diagnosis Techniques*. Springer.

Falb, P.L. and Wolovich, W.A. (1967). Decoupling in the design and synthesis of multivariable control systems. *IEEE Trans. Autom. Cont.*, 12(6), 651–659.

Frank, P.M. and Ding, X. (1997). Survey of robust residual generation and evaluation methods in observer-based fault detection systems. *J. Process Control*, 7(6), 403–424.

Glover, K. and Varga, A. (2011). On solving non-standard $H_-/H_{2/\infty}$ fault detection problems. In *Proc. of CDC and ECC'11*, 891–896.

Gumussoy, S., Henrion, D., Millstone, M., and Overton, M.L. (2009). Multiobjective robust control with HIFOO 2.0. In *Proc. of ROCOND'09*.

Ibaraki, S., Suryanarayanan, S., and Tomizuka, M. (2001). H_∞ optimization of luenberger state observers and its application to fault detection filter design. In *Proc. of CDC'01*, 1011–1016.

Isermann, R. (2005). Model-based fault-detection and diagnosis - status and applications. *Annu. Rev. Control*, 29(1), 71–85.

Jaimoukha, I., Li, Z., and Mazars, E. (2006). Fault isolation filter with linear matrix inequality solution to optimal decoupling. In *Proc. of ACC'06*, 2339–2344.

Li, Z., Mazars, E., Zhang, Z., and Jaimoukha, I. (2011). State-space solution to the H_-/H_∞ fault-detection problem. *Int. J. Robust Nonlinear Control*. Doi: 10.1002/rnc.1690.

Liu, B. and Si, J. (1997). Fault isolation filter design for linear time-invariant systems. *IEEE Trans. Autom. Cont.*, 42(5), 704–707.

Mazars, E., Jaimoukha, I.M., Li, Z., and Zolotas, A.C. (2007). Fault detection and isolation filter design for systems subject to polytopic uncertainties. In *Proc. of MEDCON'07*, 1–5.

Ostertag, E. (2008). An Improved Path-Following Method for Mixed H_2/H_∞ Controller Design. *IEEE Trans. Autom. Cont.*, 53(8), 1967–1971.

Park, J., Rizzoni, G., and Ribbens, W.B. (1994). On the representation of sensor faults in fault detection filters. *Automatica*, 30(11), 1793–1795.

Rezac, M. and Hurak, Z. (2011). Structured MIMO H_∞ design for dual-stage inertial stabilization: Case study for HIFOO. In *Proc. of IFAC WC'11*, 7456–7461.

Wahrburg, A. and Adamy, J. (2012). Robust fault isolation observers for non-square systems - a parametric approach. In *IFAC SAFEPROC'12*. Accepted.

Zhong, M., Ding, S.X., Lam, J., and Wang, H. (2003). An LMI approach to design robust fault detection filter for uncertain LTI systems. *Automatica*, 39(3), 543–550.